Control of Cross-Linking Polymerization Kinetics and Polymer Aggregated Structure in Polymer-Stabilized Liquid Crystalline Blue Phases

Takashi Iwata,[†,‡] Ken Suzuki,[†] Naoyuki Amaya,[†] Hiroki Higuchi,[§] Hiroyasu Masunaga,[||] Sono Sasaki,[||] and Hirotsugu Kikuchi*[,§]

NOF Corporation, 5-10 Tokodai, Tsukuba, Ibaraki 300-2635, Japan, Department of Applied Science for Electronics and Materials, Kyushu University, 6-1 Kasuga-koen, Kasuga, Fukuoka 816-8580, Japan, Institute for Material Chemistry and Engineering, Kyushu University, 6-1 Kasuga-koen, Kasuga, Fukuoka 816-8580, Japan, and Japan Synchrotron Radiation Research Institute, 1-1-1 Sayo-cho, Sayo-gun, Hyogo 679-5198, Japan

Received November 3, 2008; Revised Manuscript Received December 24, 2008

ABSTRACT: Kinetics of cross-linking copolymerization of acrylate- and methacrylate-monomers in a liquid crystal blue phase to prepare the polymer-stabilized blue phase were investigated based on dynamic mechanical analysis. Although the polymerization rate of methacrylate-monomers is generally much lower than that of acrylate-ones, we found that a methacrylate cross-linker enhanced the cross-linking copolymerization and an acrylate one suppressed it when acrylate- and methacrylate-monomers were copolymerized with cross-linking. The order of copolymerization rate of monofunctional monomer/difunctional one was monoacrylate (mA)/dimethacrylate (dMA), mA/diacrylate (dA), monomethacrylate (mMA)/dMA, and mMA/dA. The synchrotron small-angle X-ray scattering measurements were carried out to evaluate the aggregated structure of polymer networks in the polymer-stabilized blue phase and found the regular polymer structure corresponding to the disclination lattice of the blue phase, indicating that the polymers were segregated preferentially in the disclination cores. The degree of the regularity of polymer networks was opposite order of copolymerization rate. We obtained a good correlation among the polymerization kinetics, the mechanical elastic constant and the polymer aggregation structure in the polymer-stabilized blue phases, leading to a novel strategy to control the structure and the performance of the polymer-stabilized blue phases.

Introduction

Recently the studies of composite materials consisting of liquid crystals and polymers, such as (polymer/liquid crystal) composites,[1−3] PDLC,[4−7] liquid crystal gel,[8,9] polymer-stabilized liquid crystal structure,[10−13] and so on, have been developed rapidly and the achievements have become a center of attraction in the field of materials science. Novel phenomena and applications that cannot be achieved for pure liquid crystals are exploited by combining liquid crystals with nano- or microstructured polymer networks. Particularly the remarkable effect of the polymer networks on a stable temperature range of blue phase is worth noting. The temperature range of a blue phase of pure chiral nematic liquid crystal is known to be typically less than a few kelvin. We reported that the temperature range appearing the blue phase was extremely extended to more than several tens of kelvins by an in situ photopolymerization of a small amount of monomers in the blue phase, so-called the polymer-stabilized blue phase, and the polymers formed within the blue phase could be condensed into disclinations which coexist in the blue phase.[12] The polymer-stabilized blue phases are now noticed for their great possibilities of applications to optical device materials. A promising candidate for a next-generation liquid crystal display is now expected to be the polymer-stabilized blue phases because they show fast electro-optical response, less than 1 ms, and require no surface treatment due to optically isotropic nature.[13] The performance and durability of the polymer-stabilized blue phase are clearly dependent on the polymer network structure, which is generally created by cross-linking copolymerization of two kinds of monomer, acrylate/diacrylate dispersed in the blue phase. There is an increasing demand for controlling the polymer network structure in the polymer-stabilized blue phases. However, little is known about the factor affecting the polymer network structure in the polymer-stabilized blue phase so far, in spite of many reports about effect of polymerization kinetics on polymer aggregation structure in conventional polymer/liquid crystal composites, e.g., PDLCs.[14−22]

Here we present the experimental evidence, based on viscoelastic measurements during polymerization and synchrotron small-angle X-ray scattering, that the kinetics of cross-linking can be regulated by the monomer reactivity ratio of radical copolymerization and are the dominant factor of controlling the network structure in the polymer-stabilized blue phase.

Experimental Section

Synthesis. We synthesized various derivatives following Schemes 1 and 2. The mesogenic monomer structures were selected based on previous work.[8−13,23,24] Unless otherwise noted, Proton NMR spectra were recorded either on JEOL JNM-LA 395 (395 MHz) NMR spectrometer. Chemical shifts were reported in parts per million downfield relative to internal tetramethylsilane (TMS, δ = 0.00) or with the solvent reference as the internal standard ($CDCl_3$, δ 7.26). Data were reported as follows: chemical shift, multiplicity (s = singlet, d = doublet, t = triplet, q = quartet, o = octet, br = broad, m = multiplet), coupling constants (Hz), intergration, and assignment. Elemental analyses were performed with Yanaco MT-5 or MT-6 CHN-CORDE. All reagents were obtained from commercial sources and used without further purification.

Synthesis of 12-Iodododecyl (Meth)Acrylate[25] (1). To a solution of 12-bromododecanol (2.00 g, 7.5 mmol) and triethyl-

* To whom correspondence should be addressed. E-mail: kikuchi@cm.kyushu-u.ac.jp.
[†] NOF Corporation.
[‡] Department of Applied Science for Electronics and Materials, Kyushu University.
[§] Institute for Material Chemistry and Engineering, Kyushu University.
[||] Japan Synchrotron Radiation Research Institute.

10.1021/ma802464w CCC: $40.75
Published on Web 02/17/2009

Scheme 1

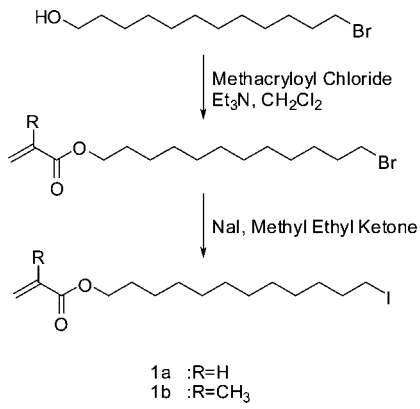

1a :R=H
1b :R=CH_3

amine (2.29 g, 22.6 mmol) in 20 mL of CH_2Cl_2 in an ice bath was added dropwise acryloyl chloride (0.68 g, 7.5 mmol). After being stirred for 20 min, the reaction mixture was then stirred overnight at room temperature. The resulting mixture was poured into water and then extracted with CH_2Cl_2. The extracts was washed with brine, dried over $MgSO_4$, filtered, and concentrated *in vacuo*. The residue was purified by flash column chromatography (SiO_2, heptane/ethyl acetate 4/1) to give 12-bromododecyl acrylate (2.3 g). A solution of the bromoacrylate (2.3 g) and sodium iodide (3.37 g, 22.5 mmol) in 40 mL of methyl ethyl ketone was refluxed for 3 h. The resulting mixture was poured into water and then extracted with CH_2Cl_2. The extracts was washed with brine, dried over $MgSO_4$, filtered and concentrated *in vacuo*. The residue was purified by flash column chromatography (SiO_2, heptane/ethyl acetate 3/1) to give 12-iodododecyl acrylate 1a (2.3 g, 93%) as yellow oil. 12-Iodododecyl methacrylate **1b** was obtained with the same reaction condition.

1a: ^{1}H NMR δ 1.20−1.40 (m, 16H), 1.64 (m, 2H), 1.81 (m, 2H), 3.15 (t, J = 6.3 Hz, 2H), 4.13 (t, J = 8 Hz, 2H), 5.78 (dd, J = 10, 1.5 Hz, 1H), 6.10 (dd, J = 10, 16.5 Hz, 1H), 6.38 (dd, J = 16.5, 1.5 Hz, 1H).

1b: ^{1}H NMR δ 1.27−1.38 (m, 22H), 1.63−1.70 (m, 2H), 1.78−1.86 (m, 2H), 1.94 (t, J = 1.2 Hz, 3H), 3.19 (t, J = 7.0 Hz, 2H), 4.14 (t, J = 6.8 Hz, 2H), 5.53−5.55 (m, 1H), 6.09 (m, 1H).

Anal. Calcd for $C_{16}H_{29}IO_2$: C, 50.53; H, 7.69; I, 33.37. Found: C, 50.82; H, 7.75.

Synthesis of 2-Methyl-1,4-phenylene Bis{4-[3-(methacryloyloxy)propyloxy]benzoate} (2). *Synthesis of Ethyl 4-(3-Hydroxypropyloxy)benzoate.* A solution of ethyl 4-hydroxybenzoate (6.64 g, 40 mmol), 3-chloro-1-propanol (3.78 g, 40 mmol), and anhydrous potassium carbonate (8.29 g, 60 mmol) in 50 mL of methyl ethyl ketone was refluxed for 48 h. The reaction mixture was then cooled to room temperature and poured into 50 mL of water. The mixture was extracted twice with 50 mL of CH_2Cl_2. The combined organic phases were dried over $MgSO_4$, filtered, and concentrated *in vacuo*. The residue was purified by flash column chromatography (SiO_2, heptane/ethyl acetate 2/1) to give ethyl 4-(3-hydroxypropyloxy)benzoate (5.38 g, 60.6%) as a white solid.

Synthesis of Ethyl 4-(Methoxymethyloxypropyloxy)benzoate. To a solution of ethyl 4-(3-hydroxypropyloxy)benzoate (4.93 g, 22.0 mmol) and diisopropylethylamine (5.69 g, 44.0 mmol) in 20 mL of CH_2Cl_2 in an ice bath was added dropwise chloromethyl methyl ether (1.95 g, 24.2 mmol). After being stirred for 20 min, the reaction mixture was stirred overnight at room temperature. The resulting mixture was poured into water and then extracted with CH_2Cl_2. The extracts were washed with brine, dried over $MgSO_4$, filtered, and concentrated *in vacuo*. The residue was purified by

Scheme 2

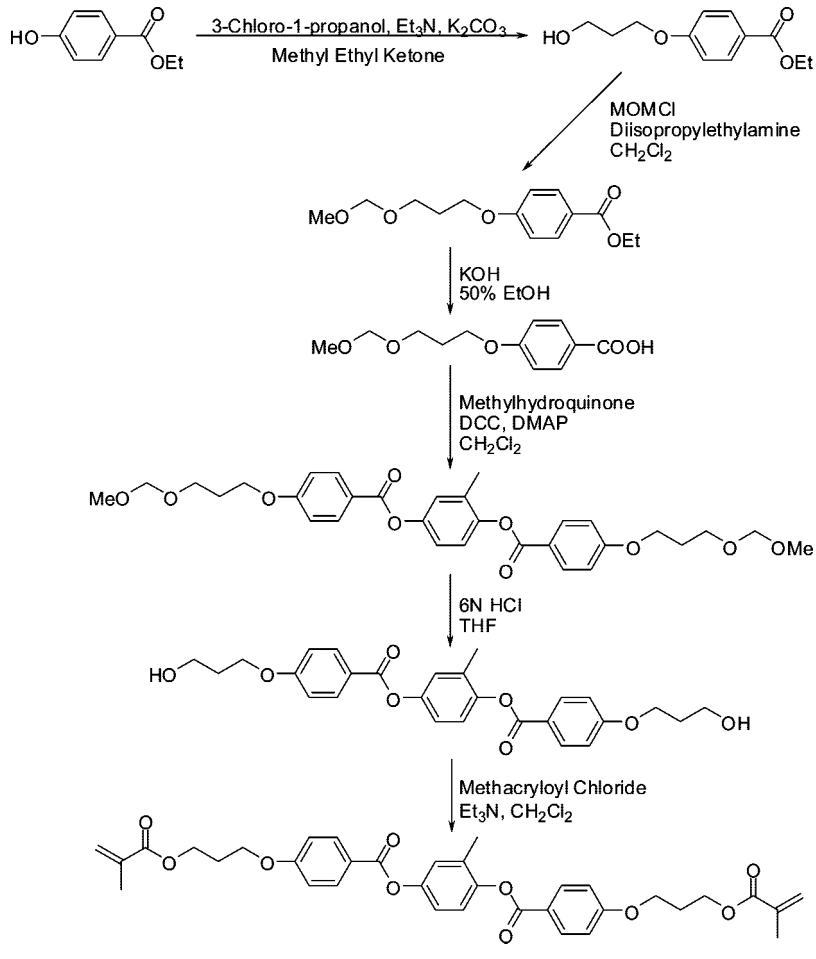

flash column chromatography (SiO_2, heptane/ethyl acetate 3/1) to give ethyl 4-(methoxymethyloxypropyloxy)benzoate (3.51 g, 71.1%) as a white solid.

^{1}H NMR: δ 1.38 (t, J = 7.2 Hz, 3H), 2.06−2.13 (m, 2H), 3.72 (t, J = 6.3 Hz, 2H), 4.13 (t, J = 6.3 Hz, 2H), 4.34 (q, J = 7.2 Hz, 2H), 4.63 (s, 2H), 6.92 (d, J = 8.7 Hz, 2H), 7.99 (d, J = 8.7 Hz, 2H).

Synthesis of 4-[3-(Methoxymethyloxy)propyloxy]benzoic Acid. To a solution of KOH (9.3 g, 165 mmol) in 100 mL of 50% ethanol at room temperature was added ethyl 4-(methoxymethyloxypropyloxy)benzoate (3.0 g, 11.2 mmol). After stirred for 48 h, the reaction mixture was treated with 30 mL of cold concentrated HCl (to pH 3). The resulting white precipitate was collected by filtration, washed with water, and recrystallized from methanol solution to give 4-[3-(methoxymethyloxy)propyloxy]benzoic acid (2.21 g, 82.0%) as colorless crystals.

^{1}H NMR: δ 2.08−2.14 (m, 2H), 3.35 (s, 3H), 3.73 (t, J = 6.0 Hz, 2H), 4.16 (t, J = 6.3 Hz, 2H), 4.64 (s, 2H), 6.95 (d, J = 8.7 Hz, 2H), 8.05 (d, J =8.7 Hz, 2H).

Synthesis of 2-Methyl-1,4-phenylene Bis{4-[3-(methoxymethyloxy)propyloxy]benzoate}. 4-[3-(Methoxymethyloxy)propyloxy]-benzoic acid (2 g, 8.3 mmol) and methylhydroquinone (0.52 g, 4.15 mmol) were dissolved into 50 mL of CH_2Cl_2. The solution was cooled in an ice bath. After the mixture was stirred for 20 min, dicycrohexylcarbodiimide (2.56 g, 12.45 mmol) and dimethylaminopyridine (0.25 g, 2 mmol) were added. The reaction solution was stirred overnight at room temperature. The resulting mixture was poured into water and then extracted with CH_2Cl_2. The extracts was washed with brine, dried over $MgSO_4$, filtered and concentrated *in vacuo*. The residue was purified by flash column chromatography (SiO_2, heptane/ethyl acetate 1/1) to give 2-methyl-1,4-phenylene bis{4-[3-(methoxymethyloxy)propyloxy]benzoate} (2.1 g, 90%) as a white solid.

^{1}H NMR: δ 2.15−2.09 (m, 4H), 2.24 (s, 3H), 3.36 (s, 6H), 3.74 (t, J = 6.0 Hz, 4H), 4.18 (t, J = 6.2 Hz, 2H), 4.19 (t, J = 6.2 Hz, 2H), 4.65 (s, 4H), 6.99 (d, J = 4.8 Hz, 2H), 7.01 (d, J = 4.8 Hz, 2H), 7.06−7.19 (m, 3H), 8.14 (d, J = 9.5 Hz, 2H), 8.17 (d, J =9.5 Hz, 2H).

Synthesis of 2-Methyl-1,4-phenylene Bis[4-(3-hydroxypropyloxy)benzoate]. A solution of 2-methyl-1,4-phenylene bis{4-[3-(methoxymethyloxy)propyloxy]benzoate} (2 g, 3.5 mmol) in 100 mL of 6 N HCl/THF (1/1 = v/v) mixture was stirred for 48 h at room temperature. The reaction mixture was extracted twice with 200 mL of CH_2Cl_2. The combined organic phases were dried over $MgSO_4$, filtered, and concentrated *in vacuo* to give a white solid. The solid was recrystalized from ethyl acetate to give 2-methyl-1,4-phenylene-bis[4-(3-hydroxypropyloxy)benzoate] (1.45 g, 87.0%) as colorless crystals.

*Synthesis of 2-Methyl-1,4-phenylene Bis{4-[3-(methacryloyloxy)propyloxy]benzoate} (**2**).* To a solution of 2-methyl-1,4-phenylene bis[4-(3-hydroxypropyloxy)benzoate] (1.5 g, 3.1 mmol) and triethylamine (0.94 g, 9.3 mmol) in 20 mL of CH_2Cl_2 in an ice bath was added dropwise methacryloyl chloride (0.71 g, 6.8 mmol). After being stirred for 20 min, the reaction mixture was stirred overnight at room temperature. The resulting mixture was poured into water and then extracted with CH_2Cl_2. The extracts was washed with brine, dried over $MgSO_4$, filtered and concentrated *in vacuo*. The residue was purified by flash column chromatography (SiO_2, heptane/ethyl acetate 1/1) to give 2-methyl-1,4-phenylene-bis{4-[3-(methacryloyloxy)propyloxy]benzoate} (0.59 g, 30.8%) as a white solid.

2: ^{1}H NMR δ 1.96 (s, 6H), 2.19−2.26 (m, 4H), 2.25 (s, 3H), 4.14 (t, J = 6.3 Hz, 2H), 4.17 (t, J = 6.3 Hz, 2H), 4.38 (t, J = 6.3 Hz, 4H), 5.58−5.59 (m, 2H), 6.12 (s, 2H), 6.98 (d, J = 5.1 Hz, 2H), 7.00 (d, J = 5.1 Hz, 2H), 7.07−7.19 (m, 3H), 8.15 (d, J = 9.0 Hz, 2H), 8.17 (d, J =9.0 Hz, 2H).

Anal. Calcd for $C_{35}H_{36}O_{10}$: C, 68.17; H, 5.88. Found: C, 67.87; H, 5.89.

Sample Preparation. Chemical structures of the reactive monomer components used are given in Figure 1. Iodo-labeled monomers, 12-iodo-*n*-dodecyl acrylate (mA, **1a**) and 12-iodo-*n*-dodecyl methacrylate (mMA, **1b**), were used as X-ray scattering components. We used two cross-linkers, acrylate derivative, 2-methyl-1,4-phenylene bis{4-[3-(acryloyloxy)propyloxy]benzoate} (dA, Merck), and methacrylate derivative, 2-methyl-1,4-phenylene bis{4-[3-(methacryloyloxy)propyloxy]benzoate} (dMA, **2**).

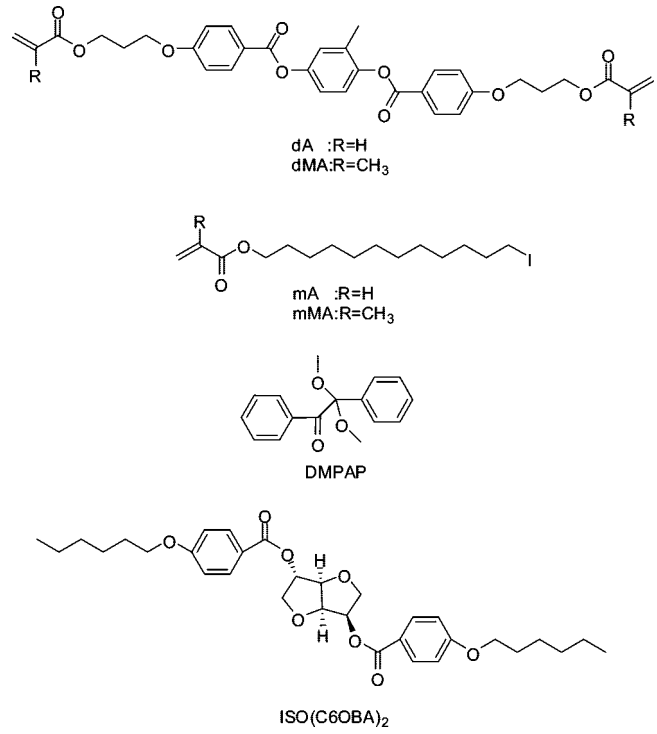

Figure 1. Chemical structures of monomers, photoinitiator, and chiral dopant.

Precursors to obtain polymer-stabilized blue phases were composed of mixtures of the nematic LC 4-cyano-4′-pentylbiphenyl (5CB, Aldrich), fluorinated nematic mixture JC1041xx (Chisso), the chiral dopant 2,5-bis-[4′-(hexyloxy)-phenyl-4-carbonyl]-1, **4**; 3,6-dianhydride-D-sorbitol ($ISO(C6OBA)_2$, synthesized[26]), iodo-labeled monomer (mA or mMA), and cross-linker (dA or dMA). These materials were homogeneously mixed in the weight ratio 42.55(5CB)/42.55(JC1041xx)/6.9(ISO(C6OBA)2)/4.0(iodo-labeled monomer)/4.0(cross-linker) and 0.4 wt % of phtoinitiator 2, 2-dimethoxy-2-phenylacetophenone (DMPAP, Aldrich) was added to the precursors.

The phase behavior of all precursors was characterized by observation of optical texture under crossed polarizer, before polymerization. Polarizing optical microscopy was performed by loading the samples into commercially available glass cells(EHC) with a polarizing optical microscope (OPTIPHOT2-POL, Nikon) equipped with heating stage(LTS-E350, Linkum), to control sample temperatures at 1 K min^{-1}.

Dynamic Mechanical Analysis. Visco-elastic properties, such as storage and loss moduli (G', G'') of sample mixtures before and during polymerization were examined by UV-rheometer (VAR-100, RHEOLOGICA Instruments AB), using a 40 mm aluminum and quartz parallel plates system, which was enclosed within a convection oven. The temperature of the sample was measured by insertion of a thermocouple on outer surface of bottom quartz plate and controlled by supplying air. A gap was maintained at 100 μm for all samples. A precursor was placed between these plates at 328 K, where all precursors were in isotropic phase. Radial shear strain and oscillation frequency were 1% and 1 Hz, respectively. These strain and oscillation amplitude were settled on relatively small values, to avoid the phase transition induced by mechanical shear flow.

Before polymerization, we have evaluated thermo-mechanical properties of all precursors to confirm the rheological features at the N*−BPI−BPII−isotropic phase transitions and determined

Table 1. Transition Temperatures and Polymerization Temperatures for Various Monomer/LC Mixtures[a]

	monofunctional monomer	cross-linker	phase transition temperature /K iso	BPII	BPI	N*	polymerization temp/K
1	mA	dA	313.7	311.7	303.8		311.2
2	mMA	dA	313.6	311.4	305.0		310.9
3	mA	dMA	312.3	310.1	301.9		309.6
4	mMA	dMA	312.0	309.9	301.8		309.4

[a] Transition temperatures were evaluated by POM observation (cooling rate 1 K/min). Each mixture is composed of 5CB/JC1041xx/ISO(C6OBA)$_2$/monofunctional monomer/cross-linker and the weight ratio is 42.55/42.55/6.9/4.0/4.0.

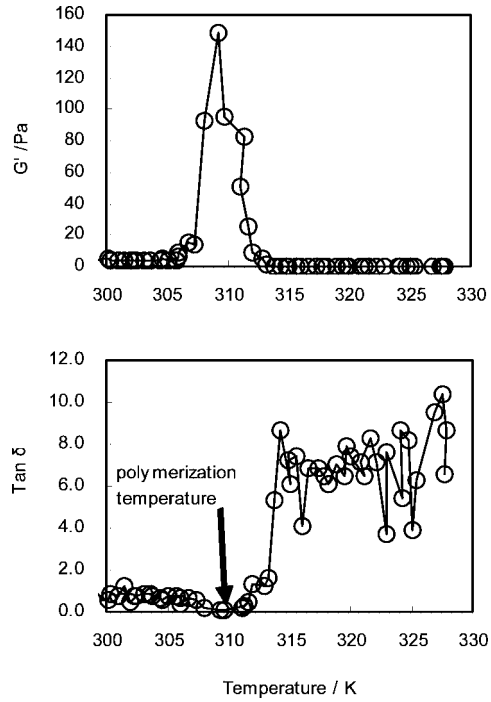

Figure 2. Temperature dependences of storage moduli G' and tan δ for monomer/LC mixture containing mA/dA monomers (cooling rate 1 K/min).

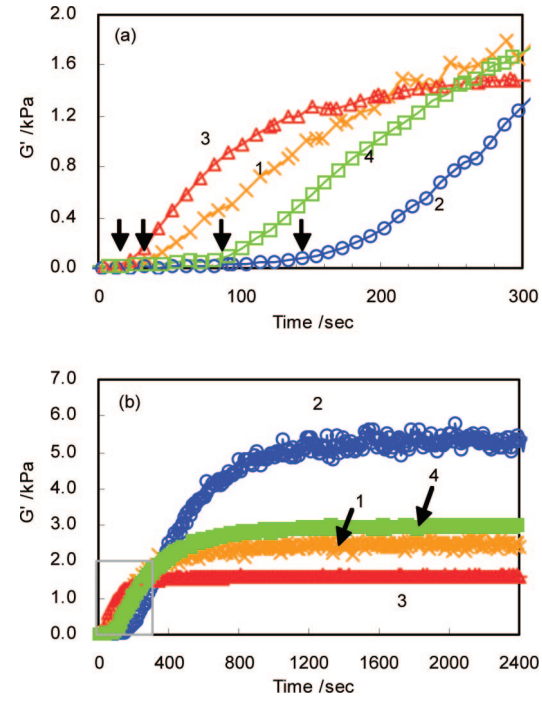

Figure 3. UV exposure time dependences of elastic constant G': for various monomer systems at (a) an early stage of polymerization (gelation times marked by arrows, respectively) and (b) overall. UV irradiation begun at 20 s.

polymerization temperatures on a UV-rheometer. Photopolymerization was performed by UV radiation from xenon lump (LIGHTNINGCURE LC5, Hamamatsu). The radiation intensity was attenuated to 1.5 mW cm^{-2} at 365 nm, UV-exposure time was 40 min. Sample temperatures were controlled at each polymerization temperatures within $\pm$0.5 K accuracy and G' and G'' were recorded during polymerization.

Synchrotron SAXS Measurements. Polymer aggregation structure in the polymer-stabilized blue phase was characterized by small-angle X-ray scattering (SAXS) measurements. The SAXS samples were loaded in sample cells sandwiched by 150 μm PET films and separated by 100 μm spacers and polymerized by UV-curing.

Polymerization temperatures of all precursors were determined as 0.5 K below the BPI-BPII phase transition temperatures. Photopolymerization was performed in a similar manner as the measurements of dynamic mechanical analyses.

The SAXS measurements were carried out at the beam line of BL40 (wavelength, $\lambda = 0.15$ nm) at SPring-8/JASRI, Japan. The camera length was 4305 mm. The exposure time of X-ray was 60 s.

Results and Discussion

Polymerization Kinetics. Two kinds of monomer, a monofunctional monomer and a difunctional one which serves as a cross-linker were used to form a polymer in the blue phase. As the functional group, acrylate and methacrylate groups were used for each monomer. Therefore totally 4 types of combination were investigated in this study, monoacrylate (mA)/diacrylate (dA), monomethacrylae (mMA)/dA, mA/dimethacrylate (dMA), and mMA/dMA. The combination of the reactive monomers in the precursor and the phase transition temperatures of the precursor evaluated by polarizing optical microscopic observation were shown in Table 1. All precursors showed similar phase sequence to one another in a similar temperature range.

In order to understand the formation process of polymer networks in the precursor, the dynamic mechanical analysis was carried out using the UV-rheometer. Figure 2 shows typical rheological behavior of the sample 1 containing a mA/dA monomer mixture on cooling process. The substantial scattering in the magnitude of tan δ at the higher temperature range is due to low viscosity of the sample, indicating that the precursor was in an isotropic liquid phase. Subsequently, G' increased rapidly and at the same time tan δ decreased to nearly zero. Further cooling, G' decreased abruptly and tan δ increased to a certain level. According to pioneering works,[27] the blue phases are known to show relatively large G' and low tan δ compared to those of N* and isotropic phase because of their three-dimensionally ordered structure. Therefore the temperature range where G' was sharply large and tan δ was low could correspond to that of the blue phase. Photopolymerization was performed at the center of bottom plateau of tan δ (marked by arrow). Although, we could not distinguish between a blue phase I and a blue phase II during dynamic mechanical measurements, all samples showed similar reflection color derived from the Bragg reflection of a blue phase I after polymerization.

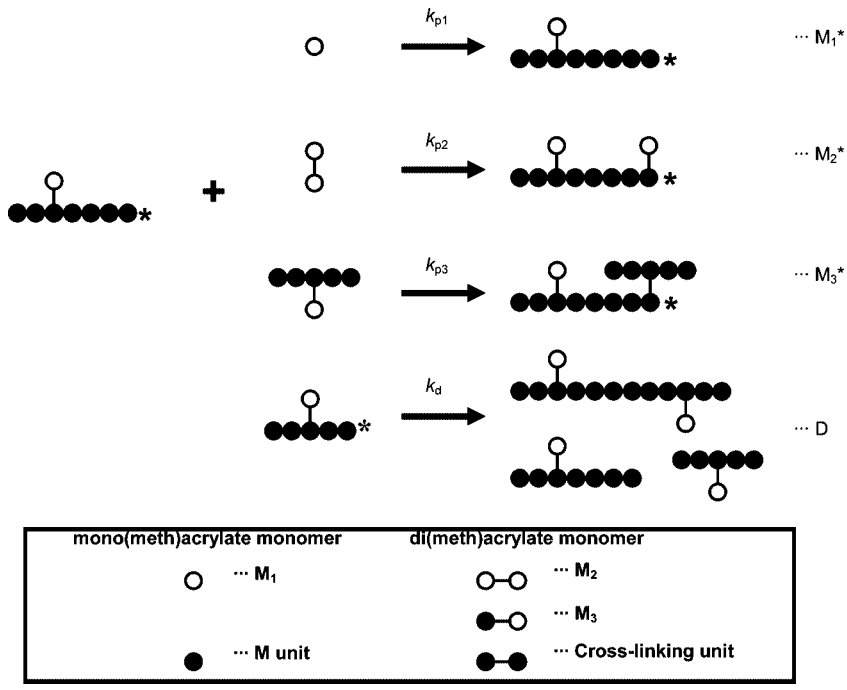

Figure 4. Schematic representation of a model of cross-linking copolymerization of monofunctional monomer and difunctional monomer.

Parts a and b of Figure 3 show the time dependence of the storage modulus, G' of the precursor during photoirradiation in a blue phase. Through the measurements, tan δ was nearly zero, indicating that the solution preserved the blue phase during dynamic mechanical measurements. In an early stage of polymerization, G' increased rapidly after a moderate rise as shown in Figure 3a. The onset times of the rapid increase of G' were different among four types of samples as sample 3 for 13 s, sample 1 for 35 s, sample 4 for 72 s and sample 2 for 124 s, respectively. In a cross-linking copolymerization, a gelation occurs if a sufficient amount of cross-linker is contained. At the gel point, an infinitely large network is formed and a mechanical modulus rapidly increases. Therefore the rapid increases of G' in Figure 3 should correspond to the gelation of polymer networks in the blue phase. Generally the polymerization rate of methacrylate-monomers is much lower than that of acrylate-ones. Interestingly, the order of the onset times indicated by arrows in Figure 3a was mA/dMA (sample 3), mA/dA (sample 1), mMA/dMA (sample 4) and mMA/dA (sample 2). That is, a methacrylate cross-linker (dMA) enhanced the cross-linking copolymerization and an acrylate one (dA) suppressed it. Let us discuss the result based on theoretical kinetic model of free-radical cross-linking copolymerization. The monofunctional monomer (mFM)-difunctional monomer (dFM) copolymerization reactions can be considered to involve at least three types of functional groups as shown schematically in Figure 4 as reported by Okay.[28] M_1 is a functional group of mFM, M_2 is that of dFM, and M_3 is a pendant functional group on a polymer chain. The instantaneous rate constants for propagation and termination reactions defined as

$$k_{pj} = \sum_{j=1}^{3} k_{pij} x_i \tag{1}$$

$$k_t = \sum_{i=1}^{3} \sum_{j=1}^{i} k_{tij} x_t x_j \tag{2}$$

$$x_j = \frac{[M_j^*]}{[R^{\bullet *}]} \tag{3}$$

where k_{pij} is the propagation rate constant between radicals M_i* and monomers M_j, k_{tij} is the termination rate constant between radicals M_i* and monomers M_j* and $[R^{\bullet *}]$ is the total radical molar concentration defined by

$$[R^{\bullet *}] = \sum_{j=1}^{3} [M_j^*] \tag{4}$$

.

The rate equations r_i for the concentration of the initiator I, functional groups M_i and cross-links μ are derived as follows:

$$r_I = -k_d[I] \tag{5}$$

$$r_{M_1} = -k_{p1}[R^{\bullet *}][M_1] \tag{6}$$

$$r_{M_2} = -2k_{p2}[R^{\bullet *}][M_2] \tag{7}$$

$$r_{M_3} = k_{p2}[R^{\bullet *}][M_2] - k_{p3}[R^{\bullet *}][M_3] \tag{8}$$

$$r_\mu = k_{p3}[R^{\bullet *}][M_3] \tag{9}$$

$$[R^{\bullet *}] = (2fk_d[I]/k_t)^{1/2} \tag{10}$$

where k_d is the decomposition rate constant of the initiator and f is the initiator efficiency.

The propagation rate of cross-linking is determined by reaction 9, which is dominated by kinetic constant k_{p3}. If dFM is a symmetrical monomer, that is, the both functional groups in dFM are same, $k_{pi3} = k_{pi2}$ and $k_{p2j} = k_{p3j}$ are approximately satisfied. In such case, when the monomer reactivity ratios hold k_{p11}/k_{p13} ($=k_{p12}$) < 1 and k_{p33} ($=k_{p22}$)/k_{p31} ($=k_{p21}$) > 1, the cross-linking reaction is clearly accelerated because k_{p3} and k_{p2} become larger, enhancing the increase of r_μ and consumption of M_2. In the case of copolymerization of acrylate monomer and methacrylate one, the monomer reactivity ratios are known to be k_{11}/k_{12} < 1 and k_{22}/k_{21} > 1, when M_1 and M_2 are acrylate monomer and methacrylate one, respectively.[29] Therefore, the cross-linking copolymerization could be speeded up if the monomer combination is the case of mA/dMA (sample 3), on the other hand, slowed down if the case of mMA/dA (sample 2) compared to copolymerizations, mA/dA (sample 1) and mMA/dMA (sample 4). The mA/dA (sample 1) copolymerization is generally faster than mMA/dMA (Sample 4). The order of the gelation times shown in Figure 3a, mA/dMA (sample

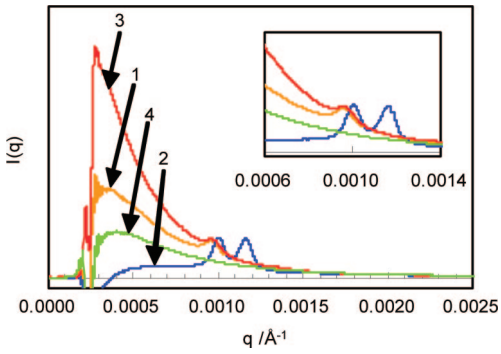

Figure 5. Synchrotron SAXS profiles for polymer-stabilized blue phases constructed from various monomers

3), mA/dA (sample 1), mMA/dMA (sample 4) and mMA/dA (sample 2), agrees completely with the order of cross-linking rates expected from their monomer reactivity ratios mentioned above.

The increases in G' were gradually saturated with UV irradiation time as shown in Figure 3b. The order of the magnitudes of saturated G's were mMA/dA (sample 2), mMA/dMA (sample 4), mA/dA (sample 1), and mA/dMA (sample 3), which are complete opposite of the order of gelation time. A possible reason for this result will be discussed below.

Synchrotron SAXS Measurements. It has been speculated that the polymers in the polymer-stabilized blue phase are condensed regio-selectively in the disclination cores which form an O^8 symmetry, a kind of body-centered cubic lattice, in the same manner of the blue phase I symmetry.[30−32] We recently presented a direct experimental evidence that SAXS from the polymers in the polymer-stabilized blue phase showed diffractions which can be assigned to the structure factor of disclination line with O^8 symmetry.[24] The monomers used for SAXS studies were labeled with iodine which has much larger scattering factor of X-ray than other atoms constituting the liquid crystal molecules and polymers. Figure 5 shows SAXS profiles for the polymer-stabilized blue phase samples that contain mA/dA (sample 1), mMA/dA (sample 2), mA/dMA (sample 3), and mMA/dMA (sample 4). The SAXS profiles were found to be different depending on the monomer combination, namely the gelation time. The scattering intensity near the direct beam was larger as the gelation time was shorter. In general, the SAXS intensity profile just around the direct beam, usually monotonous decay curve, reflects a size and a shape of scatters when the size of scatters are larger than the wavelength of incident X-ray and are distributed at random. The result shown in Figure 5 clearly indicates that larger polymer aggregates without periodical structure were formed in the blue phase as the gelation time was shorter. Furthermore, clear peaks were observed at the scattering vector $q = 0.0010$ Å^{-1} and 0.0012 Å^{-1} ($q = (4\pi/\lambda)\sin(\theta/2)$), corresponding to the Bragg diffractions form the (211) and (220) planes, respectively, of the disclination lattice in the blue phase I. The diffraction peaks were clearer as the gelation time was longer. The tendencies of decrease and increase in the monotonous scattering at the small angle and the diffractions were opposite to each other. Those two kinds of polymer aggregation structure could be responsible for the kinetics of polymerization. In the initial stage of polymerization, propagating oligomers diffuse freely around by thermal motion until the size becomes larger so that they cannot move. After gelation, the polymer-networks obviously cannot diffuse any more. If the diffusing oligomers reached to a disclination core where they should be more miscible than other highly ordered region before the size of oligomers grew up to much larger than the diameter of disclination core, they would be trapped in the disclination core, resulting in formation of polymer lattice templated by the disclination lattice. If the gelation was too fast to diffuse to a disclination, the oligomers connected to each other to form large polymer aggregates. Therefore, when the gelation is fast such as the polymerization in the combination of mA/dMA (sample 3), the large masses of polymer aggregation are formed without regular structure, while if the gelation is slow such as the case of mMA/dA (sample 2), the polymers are concentrated in the disclination cores which have a regular structure with a periodicity of about a few hundred nm. In the former case, the mechanical elasticity of the composite should be low because the connection between polymer aggregates is weak. On the other hand, the composite of later case shows large elastic constant because polymer networks are dispersed in a whole of the sample. This is the reason why the final magnitude of G' was higher as the gelation was slower.

Conclusions

We have developed a novel strategy to control the polymer aggregation structure in the polymer-stabilized blue phase based on polymerization kinetics. The reactivity ratios of the monomers in the precursors clearly affected on the kinetics of cross-linking copolymerization and on the resulting polymer aggregation structures within the polymer-stabilized blue phase. The unique dependence of gelation rate in the early stage of polymerization on the reactivity ratios of the monomers can be explained on the basis of theoretical model of free-radical cross-linking copolymerization in a monofunctional monomer and bifunctional one system. We proposed a possible process of the construction of highly ordered nanostructured polymer networks in the polymer-stabilized blue phases. Our achievement will contribute toward a material design of the polymer-stabilized blue phases which come to a current hot issue for applications to a next-generation liquid crystal display with fast response and no surface treatment.

Acknowledgment. This work was partly supported by the Japan Science and Technology Agency. We thank to Dr. K. Higashiguchi for helpful discussion.

References and Notes

(1) Kajiyama, T.; Miyamoto, A.; Kikuchi, H.; Morimura, Y. *Chem. Lett.* **1989**, *1989*, 813–816.
(2) Miyamoto, A.; Kikuchi, H.; Kobayashi, S.; Morimura, Y.; Kajiyama, T. *Macromolecules* **1991**, *24*, 3915–3920.
(3) Kikuchi, H.; Nishiwaki, J.; Kajiyama, T. *Polymer J.* **1995**, *27*, 1246–1256.
(4) Fergason, J. L. *SID Int. Symp.Dig. Technol.* **1985**, *16*, 68–70.
(5) Drzaic, P. S. *J. Appl. Phys.* **1986**, *60*, 2142–2148.
(6) Doane, J. W.; Vaz, N. A.; Wu, B. G.; Zumer, S. *Appl. Phys. Lett.* **1986**, *48*, 269–271.
(7) Drzaic, P. S. *Liquid Crystal Dispersions*; World Scientific: Singapore, 1995.
(8) Hikmet, R. A. M.; Michielsen, M. *Adv. Mater.* **1995**, *7*, 300.
(9) Guymon, C. A.; Hoggan, E. N.; Clark, N. A.; Rieker, T. P.; Walba, D. M.; Bowman, N. *Science* **1997**, *275*, 57.
(10) Yang, D. K.; Chien, L. C.; Doane, J. W. *Appl. Phys. Lett.* **1992**, *60*, 3102.
(11) Kang, K.; Chien, L. C.; Sprunt, S. *Liq. Cryst.* **2002**, *29*, 9.
(12) Kikuchi, H.; Yokota, M.; Hisakado, Y.; Yang, H.; Kajiyama, T. *Nat. Mater.* **2002**, *1*, 64.
(13) Hisakado, Y.; Kikuchi, H.; Nagamura, T.; Kajiyama, T. *Adv. Mater.* **2005**, *17*, 96.
(14) Boots, H. M. J.; Kloosterboer, J. G.; Serbutoviez, C.; Touwslager, F. J. *Macromolecules* **1996**, *29*, 7683.
(15) Nephew, J. B.; Nihei, T. C.; Carter, S. A. *Phys. Rev. Lett.* **1998**, *80*, 3276.
(16) Hoyle, C. E.; Watanabe, T. *Macromolecules* **1994**, *27*, 3790.
(17) Guymon, C. A.; Bowman, C. N. *Macromolecules* **1997**, *30*, 5271.
(18) Zhao, Y.; Chenard, Y. *Macromolecules* **2000**, *33*, 5891.
(19) Meng, S.; Duran, H.; Hu, J.; Kyu, T.; Natarajan, L. V.; Tondiglia, V. P.; Sutherland, R. L.; Bunning, T. J. *Macromolecules* **2007**, *40*, 3190.

(20) Rajaram, C. V.; Hudson, S. D.; Chien, L. C. *Chem. Mater.* **1995**, *7*, 2300.
(21) Fung, Y. K.; Ying, S.; Yang, D. K.; Chien, L. C.; Zumer, S.; Doane, J. W. *Liq. Cryst.* **1995**, *19*, 797.
(22) Chien, L. C.; Boyden, M.; Walz, A.; Shenouda, I.; Citano, C. *Macromol. Synth.* **2002**, *12*, 23.
(23) Higashiguchi, K.; Yasui, K.; Kikuchi, H. *J. Am. Chem. Soc.* **2008**, *130*, 6326.
(24) Kikuchi, H.; Izena, S.; Higashiguchi, K.; Higuchi, H.; Masunaga, H.; Sasaki, S. *The 22nd international Liquid Crystal Conference*; June 29−July 4, **2008**, Jeju, Korea.
(25) Porter, N. A.; Chang, V. H. T. *J. Am. Chem. Soc.* **1987**, *109*, 4976.
(26) Vill, V.; Fischer, F.; Thiem, J. *Z. Naturforsch. A* **1988**, *43*, 1119.
(27) Kleiman, R. N.; Bishop, D. J.; Pindak, R.; Taborek, P. *Phys. Rev. Lett.* **1984**, *53*, 2137.
(28) Okay, O. *Polymer* **1994**, *35*, 796.
(29) Brandrup, J.; Immergut, E. H. *Polymer Handbook*, 3rd ed.; Wiley Interscience; New York, 1989; Section II "Polymerization and Depolymerization".
(30) Wright, D. C.; Mermin, N. D. *Phys. Rev. A* **1985**, *31*, 3498.
(31) Keyes, P. H. *Phys. Rev. Lett.* **1987**, *59*, 83.
(32) Cladis, P. E.; Pieranski, P.; Joanicot, M. *Phys. Rev. Lett.* **1984**, *52*, 542.

MA802464W